

# Chaotic Behavior on Rocking Vibration of Rigid Body Block Structure under Two-dimensional Sinusoidal Excitation (In the Case of No Sliding)

**Man-Yong Jeong**

*Department of Electronics & Control Engineering, Numazu College of Technology, Japan*

**Hyun Lee, Ji-Hoon Kim**

*Factory Automation Research Center for Parts of Vehicles, Chosun University,  
375 Seosuk-dong, Dong-gu, Gwangju 501-759, Korea*

**Jeong-Ho Kim**

*School of Mechanical and Automotive Engineering, Suncheon National University,  
#315 Maegok-dong, Suncheon, Chonnam 540-742, Korea*

**In-Young Yang\***

*School of Mechanical Engineering, Chosun University,  
375 Seosuk-dong, Dong-gu, Gwangju 501-759, Korea*

This present work focuses on the influence of nonlinearities associated with impact on the rocking behavior of a rigid body block subjected to a two-dimensional excitation in the horizontal and vertical directions. The nonlinearities in rocking system are found to be strongly dependent on the impact between the block and the base that abruptly reduces the kinetic energy. In this study, the rocking systems of the two types are considered: The first is an undamped rocking system model that disregards the energy dissipation during the impact and the second is a damped rocking system, which incorporates energy dissipation during the impact. The response analysis is carried out by a numerical method using a non-dimensional rocking equation in which the variations in the excitation levels are considered. Chaos responses are observed over a wide range of parameter values, and particularly in the case of large vertical displacements, the chaotic characteristics are observed in the time histories, Poincare sections, the power spectral density and the largest Lyapunov exponents of the rocking responses. Complex behavior characteristics of rocking responses are illustrated by the Poincare sections.

**Key Words :** Rocking Vibration, Rigid Body Block, Energy Dissipation, Poincare Section, The Largest Lyapunov Exponents

## 1. Introduction

Many research works associated with the rocking behavior of rigid bodies have been under-

taken since the 1960's in order to investigate the rocking characteristics of rigid bodies such as tombstones and historical monuments and to determine the criteria for their overturning (Aslam et al., 1980; Tso and Wong, 1989). However, most of these works relied on the analytical predictions using the piecewise-linearized equations (Lin and Yim, 1996). In addition, these research works adopted extremely simplified rocking models such as pure-rigid models in which the damping is due to only abrupt energy loss during

---

\* Corresponding Author,

E-mail : iyyang@mail.chosun.ac.kr

TEL : +82-62-230-7170; FAX : +82-62-230-7170

School of Mechanical Engineering, Chosun University,  
375 Seosuk-dong, Dong-gu, Gwangju 501-759, Korea.  
(Manuscript Received April 15, 2002; Revised June 18, 2003)



where  $S(\theta)$  represents the signum function. The equations of the rocking motion can be expressed as follows :

$$\ddot{\theta} + p^2 \left\{ \frac{a_h}{g} \cos(\psi - |\theta|) + S(\theta) \left( 1 + \frac{a_v}{g} \right) \sin(\psi - |\theta|) \right\} = 0 \tag{5}$$

where  $I_o$  denotes the moment of inertia about the block edges and is given by

$$I_o = \frac{4mR^2}{3} \tag{6}$$

The rocking frequency of the block is defined by

$$p^2 = \frac{mgR}{I_o} = \frac{3g}{4R} \tag{7}$$

**2.2 Impact of block and base**

Assuming that there is sufficient friction to prevent sliding during the rocking and the impact stages the restitution coefficient is defined by

$$e = 1 - \frac{3}{2} \sin^2 \psi \tag{8}$$

As in Yim et. al.(1980), it is assumed that the angular velocities before and after the impact are related by

$$\dot{\theta}_2 = -e\dot{\theta}_1 \tag{9}$$

in which  $\theta_1$  and  $\theta_2$  are the angular velocities before and after the impact, respectively, and  $e$  denote the restitution coefficient.

**3. Rocking Response Analysis**

The rocking period of the block depends on the block size parameter  $R$ , as shown in Eq. (7). Therefore, the rocking frequency  $p$  becomes the most significant parameter in the rocking system. To simplify the problem, the rocking equation is normalized using  $\Theta = \theta / \Psi$ ,  $pt = \tau$  and  $\Omega = \omega / p$

$$\ddot{\Theta} + p^2 \left\{ \frac{a_h}{g} \cos \psi (1 - |\Theta|) + S(\Theta) \left( 1 + \frac{a_v}{g} \right) \sin \psi (1 - |\Theta|) \right\} = 0 \tag{10}$$

The normalized post-impact velocities of the mass center is expressed in terms of the pre-impact velocity as follows :

$$\dot{\Theta}_2 = -e\dot{\Theta}_1 \tag{11}$$

The normalized excitation forces in the horizontal and vertical directions are given by

$$a_h(\tau) = A_h \psi g \sin(\Omega_h \tau + \Phi_h) \tag{12}$$

$$a_v(\tau) = A_v \psi g \sin(\Omega_v \tau + \Phi_v) \tag{13}$$

Using a variable time-step Ralston's Runge-Kutta method, the rocking response analysis of the rigid block system is carried out to investigate the dependence of the response characteristics on the excitation as well as the system parameters such as the excitation amplitude, the excitation frequency and the restitution coefficient. The standard normalized sampling time of the numerical integration is 0.004. At the time of impact, the integration time-step is iteratively reduced by a factor of 10 each time until the normalized angular displacement became sufficiently small ( $10^{-6}$  or less). When the contact occurs (rotation angle equals zero), the transition of the rocking equation is carried out by adopting Eq. (8) as a description of the kinetic energy dissipation during the impact. The rocking response characteristics are examined by comparing the undamped system with the damped system. Here, the undamped system does not include the kinetic energy dissipation during impact, i.e.,  $e=1$ .

The chaotic rocking responses are found not only for the undamped rocking system but also for the damped rocking system excited by a two-dimensional force. The chaotic behavior is characterized by a blend of the random and unpredictable component and a certain ordered component, although the excitation is deterministic and periodic. The unpredictability arises from the rocking motion's extreme sensitivity upon the initial conditions, the system parameters and the excitation parameters. Nearby trajectories of the chaotic motion, which for infinitesimally different initial conditions diverge exponentially, lead to large differences in the long-term responses. Generally, the difference between the quasi-periodic and chaotic responses is not always obvious from the time histories and the Poincare section. In this study, the following five methods

of the chaotic analysis are used to examine the rocking responses. First, the bifurcation diagrams are created by plotting the normalized angular displacement sampled at periodic points in the rocking response for 50,000 points (after steady state has been achieved). The bifurcation diagrams are constructed with a sampling amplitude increments of 0.05 for horizontal excitation only, and the increment of 0.02 for vertical excitation with fixed horizontal excitation amplitude. Blanks (or gaps) between the amplitude increments represent the overturning of the object. The bifurcation diagram shows the variation of the rocking response characteristic and the response shape for variations in the system and excitation parameters, and it plots the normalized angular displacement against the excitation force  $\theta$  in rocking response data from 150,000 to 200,000. Second, time histories of selected individual responses are plotted to demonstrate the response characteristics. Third, the power spectral densities of the rocking responses are constructed by using time history of from 3000 to 7096 unit. These density function is also useful for examining the periodicity of the response. The periodic, quasi-periodic, and chaotic responses have a single dominant frequency, a finite number of incommensurate frequencies, and an infinite number of frequencies (i.e., a wideband spectrum), respectively. Fourth, the poincare sections are constructed by the strobe-points in the phase space for the rocking response sampled at periodic points of horizontal (or vertical) excitations. The diagram appears as a strange attractor in the case of the chaotic response, and one or more fixed points in the case of the periodic or subharmonic response. Fifth, the largest Lyapunov exponent is a quantitative measure of the divergence rate of nearby trajectories in the phase space. When the largest Lyapunov exponent is positive, the response is chaotic, whereas it is zero for periodic and quasi-periodic responses.

#### 4. Undamped Rocking Response

In order to investigate the basic behavior of the rocking system, the undamped rocking system,

which disregards kinetic energy dissipation during the impact, is initially considered. The undamped rocking system is not realistic but its behavior characteristics can still provide an insight to help understand the nonlinear characteristics of the damped rocking system. By using the stability analysis method, Yim predicted that there exists no stable periodic response for all combinations of the system and excitation parameters (Yim et al., 1980). The analytical predictions of the behavior of undamped systems have been confirmed by the numerical results. However, the confirmation that uses piecewise-linearized equation is limited to the case of the horizontal excitation only.

##### 4.1 One-dimensional excitation (Horizontal only)

In this section, in order to investigate the dependence of the rocking responses upon excitation amplitude, the numerical analysis is carried out with all other parameters fixed. The system and excitation parameters used are  $B=1$  m,  $H=4$  m,  $e=1$  and  $\Omega_h=15.708$ . As shown in the bifurcation diagram of Fig. 2, there are no stable periodic rocking responses, only quasi-periodic, chaotic and overturning responses coexist. The bifurcation diagram also shows that the maximum response amplitude increases, and overturning is more likely to occur with increasing excitation. In fact, for the normalized horizontal excitation

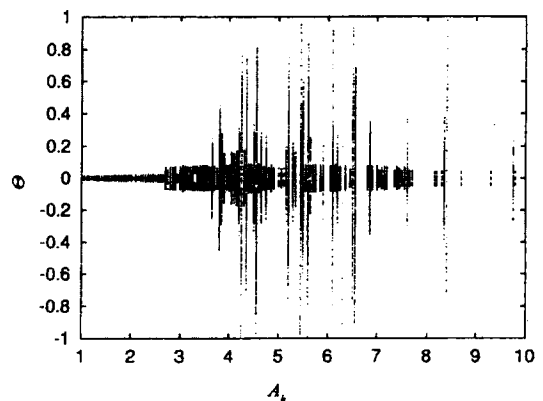
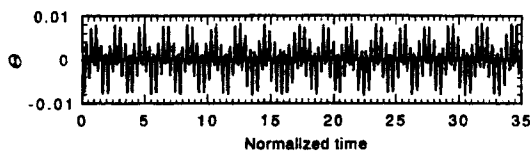


Fig. 2 Bifurcation diagram for undamped rocking responses ( $\Omega_h=15.708$ ,  $A_h=1\sim 10$ ,  $e=1$ )

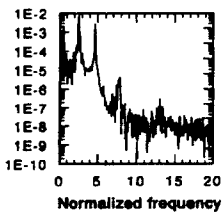
amplitude  $A_h$  less than about 3.8, the response amplitude is less than 0.1. However, it appears that overturning would likely occur for  $A_h$  exceeding 10.

The rocking responses shown in Figs. 3~6 indicate the typical chaotic responses of the undamped rocking system. The time history, the power spectral density and the Poincare section are shown in (a), (b) and (c) of these figures, respectively. As shown in these figures, the chaotic responses have aperiodic time histories and their power spectral densities contain an infinite number of frequencies. The Poincare sections shown in (c) of the above figures clearly demonstrate that the responses are chaotic. Note that

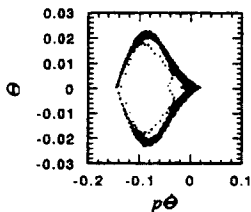
the rocking amplitude is restricted to around 0.1 in Figs. 3 and 4. Figs. 5 and 6 show the rocking responses when the excitation amplitudes are slightly different each other, namely,  $A_h=3.3957$  and  $3.3958$ . Figure 5 is an example that indicates the effect of a small variation in the excitation amplitude. For Fig. 6, the response does not show overturning, even though the excitation amplitude  $A_h$  is more than that in Fig. 5. It goes along the outward trajectory and then comes again into the inner trajectory after reaching the outer trajectory. These two responses show that the undamped rocking response can be very sensitive to small variations in the excitation parameters. The Poincare sections of all cases have the attractors of



(a) Time history

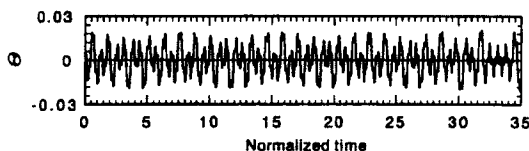


(b) Power spectra

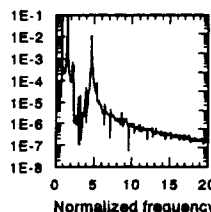


(c) Poincare map

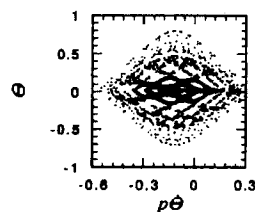
**Fig. 3** Undamped rocking response ( $\Omega_h=15.708, A_h=2.0, e=1$ )



(a) Time history

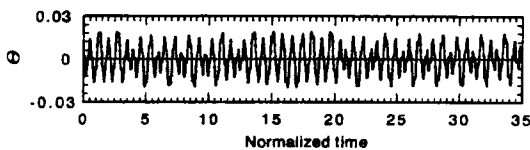


(b) Power spectra

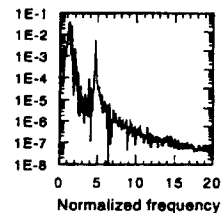


(c) Poincare map

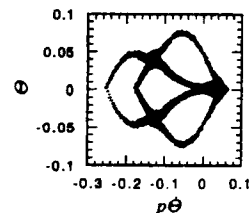
**Fig. 5** Undamped rocking response ( $\Omega_h=15.708, A_h=3.3957, e=1$ )



(a) Time history

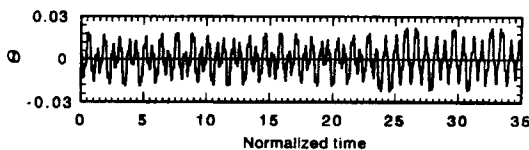


(b) Power spectra

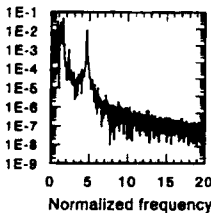


(c) Poincare map

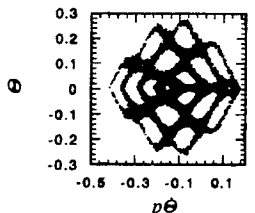
**Fig. 4** Undamped rocking response ( $\Omega_h=15.708, A_h=3.0, e=1$ )



(a) Time history



(b) Power spectra



(c) Poincare map

**Fig. 6** Undamped rocking response ( $\Omega_h=15.708, A_h=3.3958, e=1$ )

symmetric structure as shown in (c) of Figs. 3~5 when the rigid block is subjected to the horizontal excitation only. The largest Lyapunov exponents for the rocking responses are 1.5, 0.95 and 0.9 respectively. Thus it is confirmed that they are chaotic.

A typical quasi-periodic response of the undamped rocking system is shown in Fig. 7. In this case, the rocking response shows a quasi-periodic motion because the Lyapunov exponent is 0. Quasi-periodic responses can be considered to be to be a transition between the periodic and the chaotic responses. They usually appear in conjunction with the chaotic response. Thus, their appearance is indicative of an imminent chaotic response. However, no clear pattern of conditions necessary for the quasi-periodic response exists although the undamped system.

The Poincaré sections of the undamped rocking responses show a strange attractor in the phase space, which has a limit cycle of odd number and the symmetric structure. The number of the limit cycle increases or decreases depending on the variation of the excitation amplitude. The individual rocking motion about each edge contains exponentially divergent terms and is unbounded. Thus, small perturbations in the initial conditions of the rocking motions about given edge will diverge as time increases. However, the non-linearity of the transition during the impact in the undamped rocking system provides the

“folding” needed for the nonlinear (combined) rocking response to become bounded. These two elements together provide the ingredients for bounded chaotic responses. Since chaotic responses are characterized by extreme sensitivity to the system parameters nature and the transition non-linearity, they constitute a major cause of the extreme sensitivity of the rocking response.

**4.2 Two-dimensional excitation (Horizontal and vertical)**

The effects of the presence of the vertical excitation on the rocking response are examined here through a system with fixed horizontal excitation. As shown in Fig. 2, when the rigid block is subjected to a one-dimensional excitation, for  $A_h=3$ , the Poincaré points are restricted to a narrow region with  $\Theta$  less than 0.1. In this section, in order to investigate the relationship between the rocking response and the excitation amplitude in the vertical direction, the numerical analysis is carried out with the other parameters fixed. The system and the excitation parameters are  $B=1$  m,  $H=4$  m,  $e=1$ ,  $\Omega_h=\Omega_v=15.708$  and  $A_h=2$  and the vertical amplitude is varied in the increment of 0.02 from 0 to 3. The bifurcation diagram of the rocking responses for the above conditions is shown in Fig. 8. Similarly, the bifurcation diagram for the excitation parameters.  $B=1$  m,  $H=4$  m,  $e=1$ ,  $\Omega_h=\Omega_v=15.708$ ,  $A_h=3$  and  $A_v=0\sim 3$ , is shown in Fig. 9. As shown by

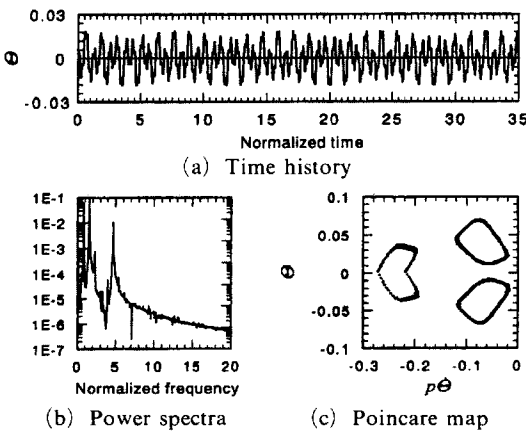


**Fig. 7** Undamped rocking response ( $\Omega_h=15.708$ ,  $A_h=3.959$ ,  $e=1$ )

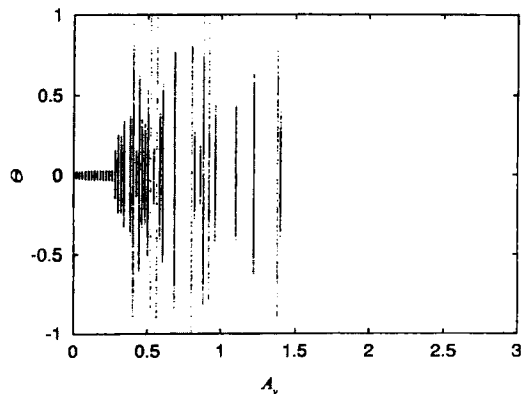


**Fig. 8** Bifurcation diagram for undamped rocking responses ( $\Omega_h=\Omega_v=15.708$ ,  $A_h=2.0$ ,  $A_v=0\sim 3$ ,  $e=1$ )

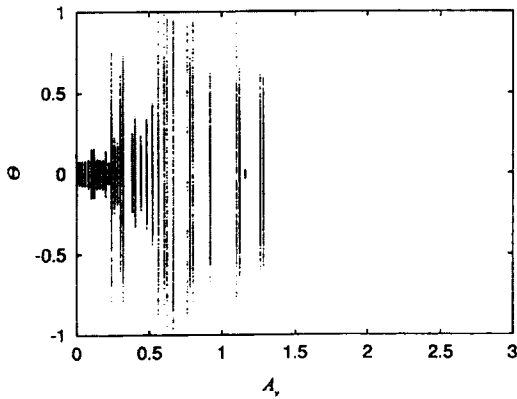
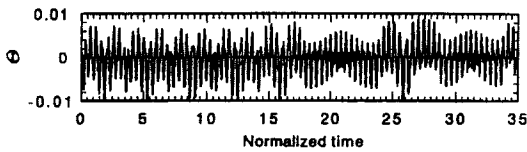
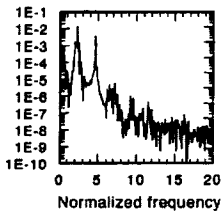


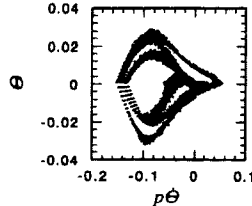
**Fig. 9** Bifurcation diagram for undamped rocking responses  
 ( $\Omega_h = \Omega_v = 15.708$ ,  $A_h = 3.0$ ,  $A_v = 0 \sim 3$ ,  $e = 1$ )



(a) Time history

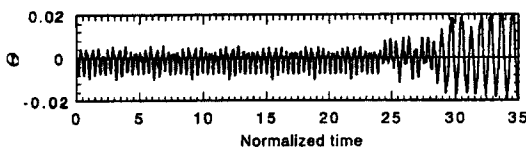


(b) Power spectra

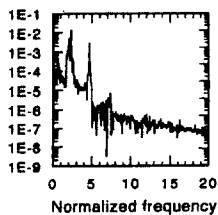


(c) Poincare map

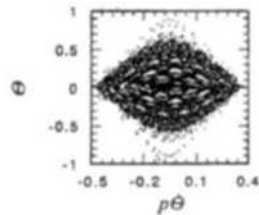
**Fig. 10** Undamped rocking response  
 ( $\Omega_h = \Omega_v = 15.708$ ,  $A_h = 2.0$ ,  $A_v = 15$ ,  $e = 1$ )



(a) Time history



(b) Power spectra



(c) Poincare map

**Fig. 11** Undamped rocking response  
 ( $\Omega_h = \Omega_v = 15.708$ ,  $A_h = 2.0$ ,  $A_v = 35$ ,  $e = 1$ )

these two bifurcation diagrams, the rocking responses become chaotic and the responses for the excitation amplitude greater than 1.25 in the vertical direction show overturning. To investigate the change of the attractor shape, examples of the undamped rocking responses for two-dimensional excitation are shown in Figs. 10~11. Fig. 10 shows the rocking response under the same conditions used in Fig. 3, except for larger vertical excitation. As shown in the Poincare section of the response, the attractor is composed of four domains of attraction that are interconnected with each other are whirl. The rocking response for  $B=1$  m,  $H=4$  m,  $e=1$ ,  $\Omega_h = \Omega_v = 15.708$ ,  $A_h = 3$ ,  $A_v = 0.35$  is shown in Fig. 11. The rocking response shown in Fig. 11 also has a periodic point group of odd numbers and diverges to the whole of phase space, which corresponds to overturning. The Poincare section has a large number of attraction domains that extend to the whole of phase space, and the power spectral density have spectrum has an infinite number of frequencies. The Lyapunov exponents for these two rocking responses are 1.1 and 0.31, respectively.

In the rocking system under the two-dimensional excitation, the dependence on the system or excitation parameters is greater than that of the one-dimensional excitation. The attractor shape of the rocking response becomes asymmetrical and more complex, and extends to wider phase space than is the case of the one-dimensional excitation. The rocking responses for the two-dimensional excitation case show a large number of attraction domains in the the whole of phase region except for a comparatively small range of the vertical excitation level. Therefore, the possibility of overturning is higher for the two-dimensional excitation case than for the one-dimensional excitation case.

### 5. Damped Rocking Response

In the previous section, the nonlinear rocking characteristics of an undamped rocking system have been explained. However, in actuality the undamped rocking system is improbable, since

the impact between the block and the base is essentially accompanied by some energy dissipation. If the block and the base are flexible and the energy dissipation during the impact is non-homogeneous, the problem will be quite complex. In this study, a restitution coefficient  $e=0.912$  is used for energy dissipation during the impact, which is determined by the geometrical condition of the block, under the assumption that both the block and the base are rigid bodies.

**5.1 One dimensional excitation**

The bifurcation diagram of the damped rocking response for  $B=1$  m,  $H=4$  m,  $\Omega_h=\Omega_v=15.708$ ,  $A_h=1\sim 10$ ,  $e=0.912$  is shown in Fig. 12. Most of the responses are periodic responses of the (1, 1) or (1, 3) mode as shown in Fig. 12, but have much more than one or three Poincare points for several excitation amplitudes. All of the responses show the periodic motion induced as a result of energy dissipation ; there is no chaotic or quasi-periodic response. However, the mode distribution of the steady-state rocking response is non-homogeneous for the excitation amplitude changes and the safety condition of the block is not easy to determine.

**5.2 Two-dimensional excitation**

The bifurcation diagram of the rocking responses for  $B=1$  m,  $H=4$  m,  $e=0.912$ ,  $\Omega_h=\Omega_v=15.708$ ,  $A_h=3$ ,  $A_v=0.35$  is shown in Fig. 13, and

the bifurcation diagram for  $B=1$  m,  $H=4$  m,  $e=0.912$ ,  $\Omega_h=\Omega_v=15.708$ ,  $A_h=4$ ,  $A_v=0.35$  is shown in Fig. 14. The bifurcation shown in Fig. 13 apparently indicates a period-doubling bifurcation for the vertical excitation amplitude less than 2.15, but shows an intermittency transition into a chaotic response for the excitation amplitude from 2.15 to 2.6. The responses show chaotic motions for some vertical excitation amplitudes, but they coexist with the periodic responses. In the case of Fig. 14, the attraction domain of the Poincare section for the vertical excitation amplitude of over 2.7 diverges to a wider region, and the response becomes chaotic. The periodic, chaotic and overturning responses

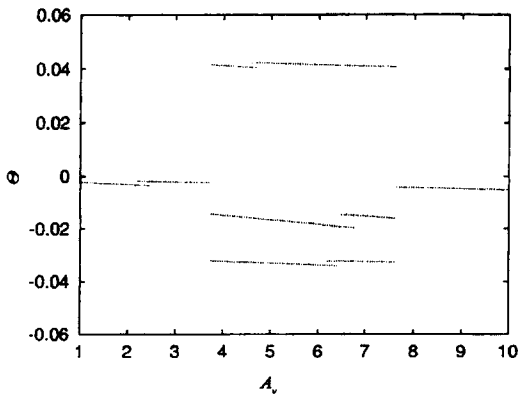


**Fig. 12** Bifurcation diagram for damped rocking responses ( $\Omega_h=15.708$ ,  $A_h=1\sim 10$ ,  $e=0.912$ )

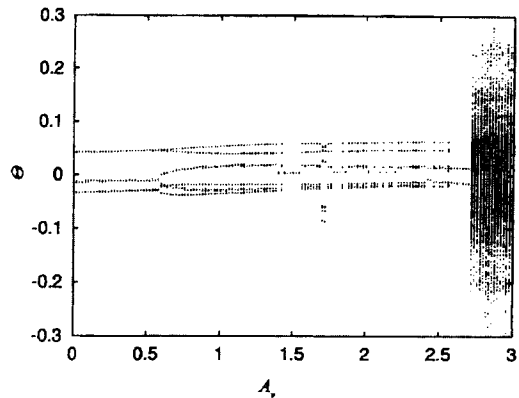


**Fig. 13** Bifurcation diagram for damped rocking responses ( $\Omega_h=\Omega_v=15.708$ ,  $A_h=3.0$ ,  $A_v=0\sim 3$ ,  $e=0.912$ )

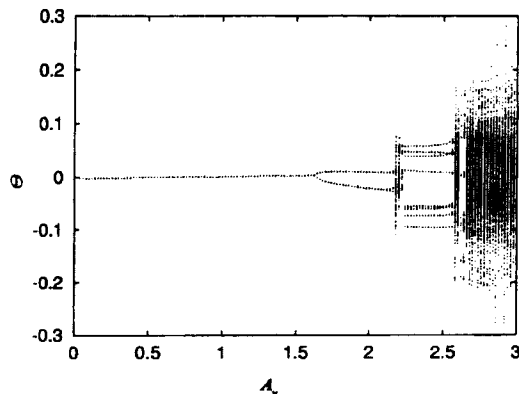


**Fig. 14** Bifurcation diagram for damped rocking responses ( $\Omega_h=\Omega_v=15.708$ ,  $A_h=4.0$ ,  $A_v=0\sim 3$ ,  $e=0.912$ )



coexist for the vertical excitation amplitude of over 2.7. Typical examples of periodic rocking responses are shown in Figs. 15~17 where (a), (b) and (c) denote the time history, the power spectral density and the Poincare section, respectively, for the rocking response. Here, the power spectral density of the rocking response is obtained from the time history after the normalized time of 25 has elapsed.

The rocking response shown in Fig. 16 passes through a long transient motion and reaches the periodic steady state rocking response in the (1, 2) mode. In this case, the Poincare section has two fixed points at first sight but it consists of two neighboring fixed points. This type of the

response can be considered to be a rocking mode in the transition or critical region between the (1, 2) and (1, 4) modes. The chaotic attractor shown in (c) of Fig. 16 consists of three fixed points, namely, the rocking response may be considered to be a periodic motion in the (1, 3) mode. The Poincare section of Fig. 16 shows the start of double period bifurcation from the two neighboring fixed points. Therefore, the response has become the periodic rocking response in the (1, 6) mode through a small increase in the excitation amplitude. Fig. 17 shows an example of the rocking response consisting of two separate fixed points. The Lyapunov exponents for these responses are 0. As shown in Figs. 13~14, the rocking response in the modes (m, n) of odd periodicity becomes the modes (m, 2m) of even periodicity through a period doubling bifurcation.

Examples of the chaotic responses are shown in Figs. 18~19. The Poincare sections for these chaotic responses show the strange attractors of the asymmetric shape, which consist of the even number of attraction domains and are whirled in the anti-clockwise direction. Note that the attractors shown in the Poincare sections for the undamped rocking responses of Figs. 10 and 11 are symmetric. This point is illustrated by comparing the above examples with one-dimensional rocking responses that cause of whirl structure is in the addition of vertical excitation as the same

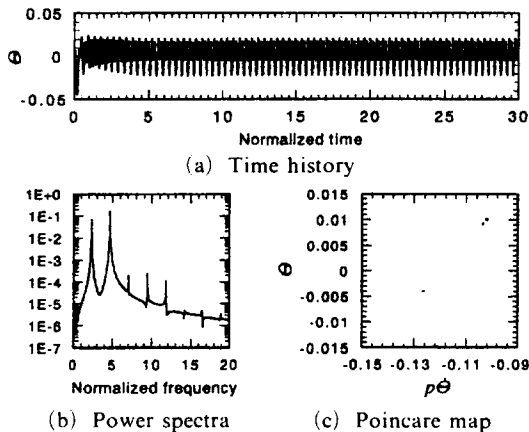


Fig. 15 Damped rocking response ( $\Omega_h = \Omega_v = 15.708$ ,  $A_h = 3.0$ ,  $A_v = 1.7$ ,  $e = 0.912$ )

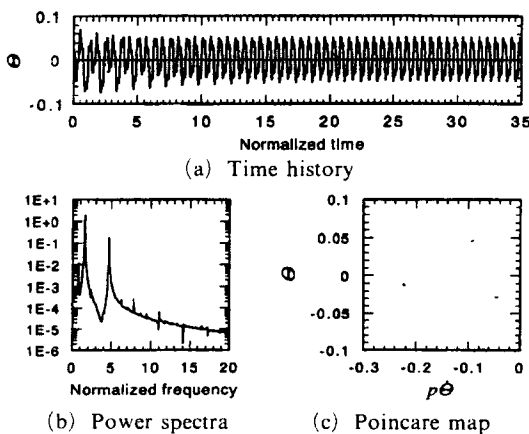


Fig. 16 Damped rocking response ( $\Omega_h = \Omega_v = 15.708$ ,  $A_h = 4.0$ ,  $A_v = 0.3$ ,  $e = 0.912$ )

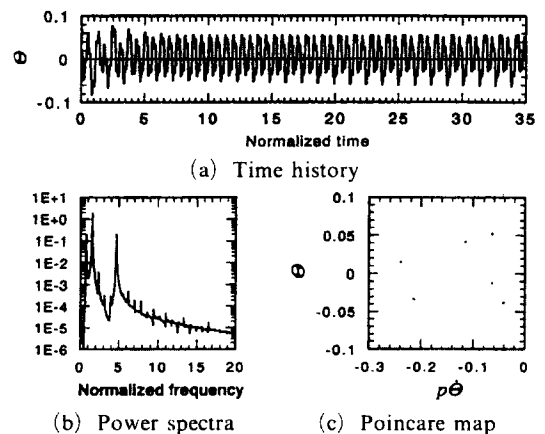


Fig. 17 Damped rocking response ( $\Omega_h = \Omega_v = 15.708$ ,  $A_h = 4.0$ ,  $A_v = 0.85$ ,  $e = 0.912$ )

way with the case of the undamped rocking system. The whirling degree of chaotic attractor is influenced by the ratio of the excitation amplitudes of the horizontal and vertical directions. The chaotic attractor shown in Fig. 18 has six domains of attraction and the attractor shown in Fig. 19 has more. The Lyapunov exponents of these chaotic responses are 1.52 and 0.98, respectively. The damped rocking response due to a one-dimensional harmonic excitation in the horizontal direction appears as a periodic motion. However, when the rocking system is subjected to a two-dimensional harmonic excitation, in both the horizontal and vertical directions, the responses are significantly influenced by the

vertical excitation and appears as the rocking responses that are either high-order rocking mode or chaotic. In particular, the rocking responses strongly depend on the excitation parameters and most of them show chaotic motion or overturning for the two-dimensional excitation case.

### 6. Initial Sensitivity

The sensitivity of the rocking response on the initial conditions is investigated by comparing the three responses with small differences in the initial conditions. The effect of the divergence of nearby trajectories on the behavior of nonlinear

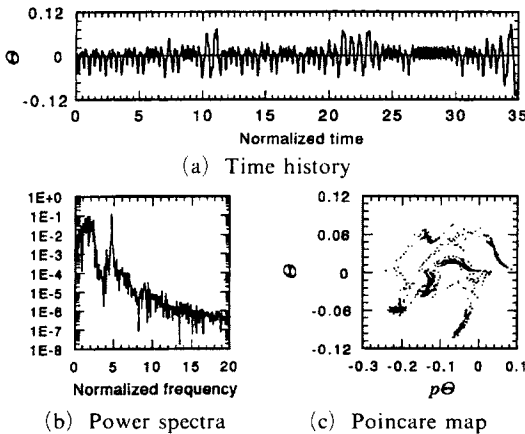


Fig. 18 Damped rocking response ( $\Omega_h = \Omega_v = 15.708, A_h = 3.0, A_v = 2.3, e = 0.912$ )

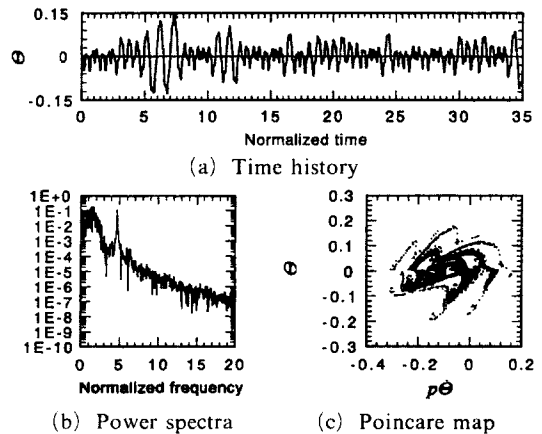


Fig. 20 Damped rocking response ( $\Omega_h = \Omega_v = 15.708, A_h = 4.0, A_v = 2.8, e = 0.912, \theta_0 = 0.00004$ )

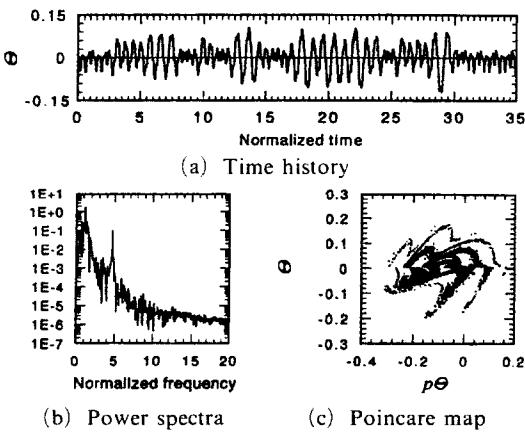


Fig. 19 Damped rocking response ( $\Omega_h = \Omega_v = 15.708, A_h = 4.0, A_v = 2.8, e = 0.912$ )

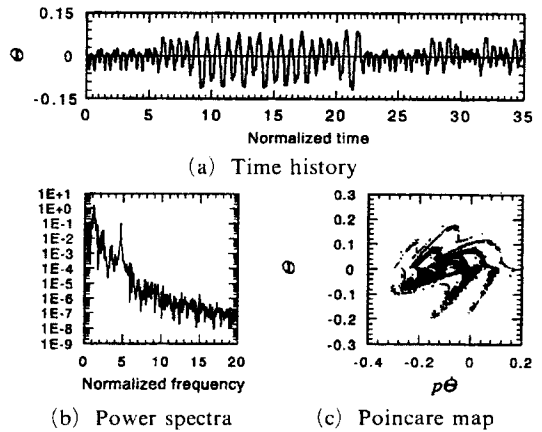


Fig. 21 Damped rocking response ( $\Omega_h = \Omega_v = 15.708, A_h = 4.0, A_v = 2.8, e = 0.912, \theta_0 = 0.00001$ )

systems can be illustrated by expressed in an elegant metaphor known as the butterfly effect. Figs. 20 and 21 show the rocking responses for the normalized initial angular displacements of  $\theta_0=0, 0.00004, \text{ and } 0.0001$ , respectively. As shown in (a) of these figures, the time motion histories are nearly identical before they reach the normalized time of 3 but become very different from each other thereafter, indicating that the rocking responses are sensitive to variations in the initial condition. However, the Poincare sections shown in (c) of Figs. 20 and 21 form the strange attractors of the identical shape, which indicate that the rocking responses are changed by small change in the initial condition, but the attractor shape of the chaotic responses is unaffected by the initial condition.

## 7. Conclusions

This study examines the chaotic behavior of the rocking response of a block shaped structure to a two-dimensional harmonic base excitation. The effects of the two types of nonlinearity in the rocking system, namely, the transition of the governing equations and energy dissipation during the impact are examined in detail. The dependence of the rocking response upon the excitation parameters is examined by using bifurcation diagrams. The results of the numerical analysis led to the follow conclusions :

(1) The response of the undamped rocking system shows chaotic motion in almost the whole phase space, except for a small region showing quasi-periodic motion. The undamped rocking response has the domains of attraction of odd number for the case of the one-dimensional excitation in the horizontal direction, but for the case of two-dimensional excitation in the horizontal and vertical directions, it has the domains of attraction of even number. The domains of attraction are connected to each other and can be made to increase or decrease by varying of the excitation amplitude or frequency. The attractors have the characteristic shapes, which whirl in the anti-clockwise direction.

(2) The response of the damped rocking sys-

tem shows periodic motions of odd periodicity such as the (1, 1) mode or the (1, 3) mode for the case of one-dimensional excitation. However, two types of rocking responses, namely, periodic responses of odd periodicity in the (1, 1) or (1, 3) mode, periodic responses of even periodicity (1, 2), (1, 4) or (1, 6) mode and the chaotic responses coexist for the case of the two-dimensional excitation in the horizontal and vertical directions.

(3) When the damped rocking system is subjected to a vertical excitation of comparatively high amplitude, the rocking response becomes chaotic motion and the attractor of the response has complex structure, and whirl in the anti-clockwise direction.

(4) The bifurcation diagrams of the undamped and damped rocking systems show the intermittency transition of the rocking response. The quasi-periodic response, the chaotic response and overturning coexist and there is no periodic response for the undamped rocking system. On the contrary, the periodic response, the chaotic response and overturning coexist for the damped rocking system when the rigid block is subjected to a two-dimensional excitation.

## Acknowledgment

This study was supported by a research grant from Chosun University, 2001.

## References

- Aslam, M., Godden, W. G. and Scalise, D. T., 1980, "Earthquake Rocking Response of Rigid Bodies," *Journal of Engineering Structure, ASCE*, Vol. 106, No. 2, pp. 377-392.
- Jeong, M. and Suzuki, K., 1995, "A basic Study on the Dynamic Behaviour of Rocking Rigid Body Structure," *Asia-Pacific Vibration Conference*, Vol. 1, pp. 365-370.
- Lin, H. and Yim, S. C. S., 1996, "Nonlinear Rocking Motions Overturning Under Random Excitations. I," *Journal of Engineering Mechanics, ASCE*, Vol. 122, No. 8, pp. 719-727.
- Lin, H. and Yim, S. C. S., 1996, "Nonlinear

Rocking Motions Overturning Under Random Excitations. II," *Journal of Engineering Mechanics, ASCE*, Vol. 122, No. 8, pp. 728~735.

Solomon, C. S. Yim and H. Lin, 1991, "Non-linear Impact and Chaotic Response of Slender Rocking Objects," *Journal of Engineering Mechanics*, Vol. 117, No. 9, pp. 2079~2100.

Spanos, P. D. and Koh, A. S., 1984, "Rocking of Rigid Blocks due to Harmonic Shaking," *Journal of Engineering Mechanics Div., ASCE*,

Vol. 110, No. 11, pp. 1627~1642.

Tso, W. K. and Wong, C. M., 1989, "Steady State Rocking Response of Rigid Blocks, Part I: Analysis," *Earthquake Engineering & Structure Dynamics*, Vol. 18, No. 106, pp. 89~106.

Yim, C. S., Chopra, A. K. and Penzien, J., 1980, "Rocking Response of Rigid Blocks to Earthquakes," *Earthquake Engineering & Structure Dynamics*, Vol. 8, No. 6, pp. 565~587.